Operationalization of an AMAN system: arrival procedures adherence study

Teresa Reis
teresa.d.reis@ist.utl.pt

Instituto Superior Técnico, Lisboa, Portugal

November 2015

Abstract

Every Area Navigation (RNAV) flight has a flight plan includes a pre planned route for approaching the airport for landing. This route is called a Standard Arrival Route (STAR) and is defined by a set of fixed points for the aircraft to follow. The Terminal Maneuvering Area (TMA) structure of an airport contains a set of STARs that ensure incoming traffic's expedition.

This thesis was developed under a protocol established between NAV Portugal and Instituto Superior Técnico. It studies aircraft's adherence to their arrival procedure, the STAR. Ultimately it aims to assist on the redesign of the TMA sector in order to best integrate the Arrival Manager (AMAN) into the system or to simply create a more efficient, flexible and dynamic airspace structure.
Keywords: AMAN, STAR, TMA, Airspace Design, Statistical Analysis

1. Introduction

Arrival Management (AMAN) systems are controllers support tools. They are intended to help air traffic controllers to efficiently manage incoming flights in order to make best use of available runway and airspace capacities. Specifically, the AMAN systems provide an aircraft sequence and an expected or scheduled time for each flight at the runway or at/over different fixes.
These systems have been developed all accross Europe since the late 1990's. According to the Local Single Sky Implementation (LSSIP) document for Portugal 2014, both the AMAN tools implementation as well as the AMAN/OSYRIS integration into LISATM are expected by the end of 2018. [3]

Traffic in Lisbon's Flight Information Region (FIR) increased by 4.3% during 2015 (January to June) when compared to the same period of 2014. In the year before the increase was of 7.5% and a baseline growth is predicted for the upcoming years. With traffic, delays have also increased and it is estimated that 99% of them were caused by Air Traffic Control (ATC) capacity and staffing. [1] AMAN intends to decrease holding, low level vectoring and consequently delays to a minimum.

Air Traffic Management (ATM) is a system composed of many interacting elements: people, procedures and equipment. Implementing a software system element such as an AMAN needs to consider all these elements. The airspace and environment in which AMAN will be used and the procedures for its use have to be considered either previously or at the same time. [5]

AMAN provides an Estimated Time of Arrival (ETA) afforded by fixed routing. In the Terminal Maneuvering Area (TMA), when approaching the airport for landing, the aircrafts follow a pre planned Standard Arrival Route (STAR). This work studies aircrafts adherence to this route. Ultimately it aims to assist airspace designers, airspace planners, controllers and the AMAN development team to come together and best redefine the TMA sector, if need be.

An analysis methodology was developed and a program in Python was created to apply it on a data set. The data includes surveillance and flight plan information from the months of March, April and May on Lisbon's FIR.

2. State-of-the-art

The TMA sector is a designated area of controlled airspace surrounding an airport. Regarding incoming traffic, there are several methods that can be employed for channeling aircrafts to a runway. Different methods imply different structuralization of the sector.

All the methods and structures presented in this chapter are eligible to be integrated into the AMAN system.

2.1. Standard Arrival Routes (STARs)

A STAR is a standard Air Traffic Services (ATS) route identified in an approach procedure by which aircraft should proceed from the en-route phase to an initial approach fix. STARs were created with the object of safe and efficiently expedite flow of air traffic operating to an airport. They aim to deconflict traffic by the use of specific routings, levels and check points. Each runway should have a number of STARs that ensures that air traffic is not unnecessarily delayed by deviation from its route. Prior to take off, every flight has a flight plan. However, the STAR field is a lot of the times left empty. In Portugal, when the flight enters the destination FIR, a STAR is automatically assigned to it by the LISATM system. The controller can then transmit that information to the flight or not. If the controller does not follow the automatic attribution by LISATM, this information can not be updated into the system, i.e. if the controller assigns a different STAR to the flight, the STAR field in the flight plan is not updated. The TMA structure of an airport contains a set of STARs that ensure incoming traffic's expedition.

2.2. Point Merge

Point Merge is an innovative method for merging arrival flows. It comes outlined in Fig.1. Incoming traffic is placed onto defined arcs, every point on which is equidistant from the runway. When cleared for landing, the aircraft make one single turn and fly a continuous descent to the runway. At the merging point, the sequence is already integrated.

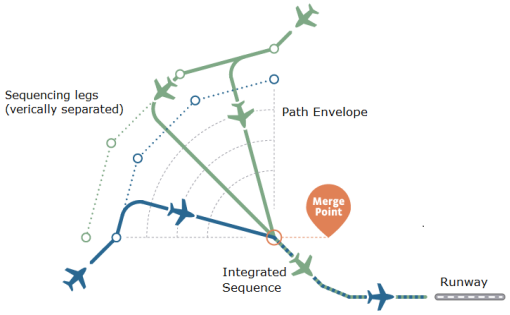

Figure 1: Point Merge.

This system eliminates the need for vectoring or stacking, reduces the need to place aircrafts into traditional holding patterns and the continuous descent approach allows for more efficient fuel usage. If there is a runway congestion, the system holds the aircrafts at much higher altitudes in the linear arcs which consequently decreases fuel burn. From the controller viewpoint, they can also benefit from enhanced situational awareness and reduced radio frequency transmissions, both of which increasing availability for tactical instructions.

Point Merge is now operational in Oslo and three Norwegian regional airports, Dublin, Seoul, Paris, Kuala Lumpur, Lagos, Canary Islands and Hannover. During 2013, it has provided savings of € 5.5 million to airlines flying into Dublin's airport.

2.3. Tactical Shortcut Options

Recent work introduced the concept of using tactical shortcut options to improve schedule conformance in the TMA. [6]

This concept consists of having a dynamic airspace structure for the TMA: longer and shorter nominal paths. If the airspace is less congested, aircrafts are scheduled the shorter paths. When a destination is congested, aircrafts are assigned the longer paths, holding the shorter paths for tactical use when an aircraft is late. Every flight has a scheduled time of arrival (STA) at coordination points along its nominal route. With the use of an AMAN, the STAs are spaced at a given point to achieve the minimum required spacing plus an additional scheduling buffer to account for uncertainty. The tactical shortcuts are assigned to late aircrafts at some point prior to a coordination point.

This concept has yet to be put into practice but claims that using fixed paths produces more accurate trajectory predictions. On the other hand, speed controlling is more efficient fuel wise than vectoring. Using fixed paths and speed control options, a more precise scheduling and tighter spacing is achieved. Though reducing flexibility, it ultimately increases throughput.

3. Implementation

The program works in two separate steps: The first step is to process and load all the data into files. Taking the processed data, the second step is to run it through algorithms and produce the desired results.

We were provided data from FDPS and Surveillance Data Processing system (SDPS) in rfm format. External software already developed at NAV was used to convert it to txt format.

3.1. Loading

With the flight data in a readable format, the processing stage could now begin.

DataSurv and DataFDPS The first step was loading the data into two GeoJSON files: DataSurv and DataFDPS.

The GeoJSON format was deliberately chosen due to two other tools: **Shapely** and **QGIS**. Shapely is a Python package for manipulation and analysis of geometric planar objects. GeoJSON files can be easily read and loaded into shapes using this package. This will be a great advantage on the testing phase. QGIS is a free and open source appli-

cation to display geographic information. It provides data viewing, editing, and analysis capabilities. The geojson files can automatically be loaded into GIS and an interactive geographical display of them is made possible.

Before tackling the flight data, additional information regarding waypoints and STARs had to was extracted and loaded.
We were now able to create DataSurv and DataFDPS. These files contain all the information from the raw SDPS and FDPS files, correlated with the waypoints and STARs data. Each file corresponds to one day and each feature within the file corresponds to one flight. Only the flights landing at the desired airport were gathered.

corData To improve efficiency, a third GeoJSON file was created: corData. This file seeks the information for the same flight in both DataSurv and DataFDPS and combines it into one single feature. Again, each corData file corresponds to one day and each feature within the file corresponds to one flight, now with all its information. The latter include Call Sign, Flight Plan (FP) key, surveillance coordinates, the FP STAR, among others.

3.2. Getting Results
Four main tests were computed. The first two test trajectorie's adherence to a STAR in 2D and 3D. The third one traces common patterns from real trajectories, aiming to create an alternative route. The last one studies direct flights.

3.2.1 2D Adherence

Taking the STAR assigned in a flight's FP, we wanted to study trajectorie's adherence to it.

Relying on the shapely tools, a buffer is drawn around the STAR. The STARs adherence rate is directly proportional to the portion of the trajectory that intersects that buffer. The buffer is set on a scale of one nautical mile and goes from 1 to 5nms to each side. Fig.2 is a QGIS representation of TAP473's flight on the INBOM3B STAR using a 2nm buffer radius.

Figure 2: TAP473 flight on the INBOM3B STAR on 2015/04/25.

In addition to the analysis of the adeherence to the STAR in its entirety, the STAR was also broke into segments. Each segment joins two consecutive points of a STAR. The adherence for each segment is tested using the same methodology as for the entire STAR.

Furthermore, an additional feature of corrections was installed. It was found that some flights showed favorable adherence results for different STARs other than the ones in their flight plan. We called these new STARs the corrected STARs. All the programs can present results for the uncorrected and/or the corrected STAR.

3.2.2 3D Adherence

The 3D analysis ceased to be as linear as the 2D since Shapely does not operate with the third coordinate z. [4] In 2D, intersecting the track in the buffed shape and getting its length required two shapely functions: intersection and length. In 3D, the exact same functions were used. However, this time it was necessary to do this proccess twice: once for $x-y$ and the other time for $l-z$, l being the length of the track and z its altitude. Getting $l-z$ involved manipulating existing geometric shapes.

Once the $x-y$ intersection was completed, the intersected track was manipulated and intersected again, this time in $l-z$. For this an auxiliary line was used. Its coordinates were: x the cumulative length of the tracks points and y the z coordinates from the track. At the same time, a polygon representing the intersection plane is built (Fig.3). Its height restrictions h_{max_A} and h_{min_B} are imposed by STAR's regulations. l_{max} is the tracks cumlative lenght.

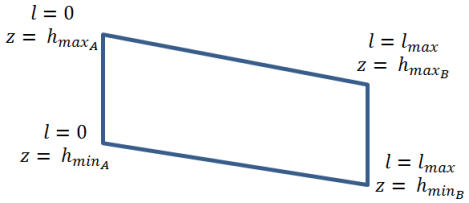

Figure 3: Height Polygon.

The end result is an intersection of both plane's results.

3.2.3 Average STARs

This test takes all the data provided and traces common trajectory patterns for each STAR. Three trajectory patterns were extracted for each STAR, each of them using a different algorithm.

Average Taking all the first points, the average first point is computed. The average point is the one

resulting from the average latitude plus the average longitude from all the points considered. The process is repeated for all the points the tracks were divided into. In the end, all the average points are joint and the average line or track for that specific STAR is obtained.

Figures 4, 5 and 6 demonstrate the process. A sample of four different tracks related to the same STAR were gathered. The segments from two consecutive normalized points from each STAR are presented in Fig.4. The average points for each set of track points are presented in red in Fig.5. In Fig.6, joining these two points, the average line segment is obtained.

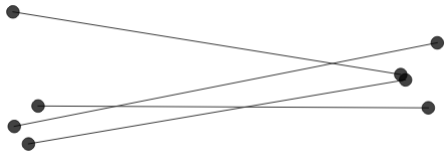

Figure 4: Sample of four track's normalized segments.

Figure 5: Computation of the average points.

Figure 6: Computation of the Average line.

Iterative Weighted Average Even though the previous test already gave successfull visual results, we wanted to further refine the pattern. For most STARs, tracks did not deviate significantly from the average. However, some STARs had one clear pattern and then a small percentage of tracks significantly different from this pattern. Computing the average was attributing the same weight to the tracks in the clear pattern and the abnormal tracks.

The Iterative Weighted Average test was built. The same normalized tracks and computed average points were considered. Taking all the first points of the tracks, its distance to the average first point is calculated. This time the computed point is the weighted average point. The weights being inversely proportional to the distance of the point to the average point. This process is done iteratively. Taking the new computed point, the distance is again calculated for each point and either is the final weighted average point. The iteration stops when the distance between new calculated points is less than $1m$. This way, the further a certain track is to the average, the less weight it will have on the new line's computation.

Continuing with the same example, in Fig.7 there is a visual comparison of the two tests. The red line results from the Average and the green from the Iterative Weighted Average test. With the refined Weighted Average test, the computed line follows the areas with bigger density of points, as desired.

Figure 7: Comparison between the Average test in red and the Iterative Weighted Average in green.

Median Lastly it was noticeable that, although more accurate than the first one, the new test resulted in a very irregular line. Furthermore, the iterations made the program heavy and slow.

In order to surpass these issues, a simpler test came to mind: the Median. Instead of joining the average points, the line is the union of the median points. On 8, the similarities between the median in yellow and the weighted average in green are identifiable. This solution results in a much smoother line and it is faster proccessing, despite the results being very similar to the last test.

Figure 8: Comparison between the iterative weighted average test in green and the median in yellow.

One could call the resulting lines new alternative STARs. An additional study was made on how much of an improvement to the real STAR these lines would be. The 2D adherence was again tested, now for the Average, Iterative Weighted Average

and Median "STARs".

3.2.4 Point Direct

This study aimed to find the percentage of cases where pilots are granted direct flights. It calculates how many flights flew a straight line for each STAR and for each STAR point.

The algorithm is as follows. Taking one non conformative flight and its STAR, it checks if the track intersects the STAR's points, starting with the point closest to the runway, one at a time until the penultimate point. If the track is positive to fly by a certain point, directivity is checked, i.e. if the trajectory until that point was a straight line. If it was not, the proccess is repeated for the next point. If it was, the results are gathered and the test continues for the next track.

3.3. Visualization

Two platforms were used for visualizing results: pdf and QGIS. The output pdf files give tabled information on adherence percentages for the entire STAR and segmented, for the uncorrected and corrected STAR. In Point Direct, the pdf file provides tabled data for all the direct flights to all the STARs and STAR points. The output QGIS files interactively demonstrate the tracks, the STARs and their segments.

4. Results

For this work 3 months of Surveillance Data Processing System (SDPS) and FDPS data were provided: March, April and May of 2015. This data covered Lisbon's FIR which includes the continental area and Madeira.

The main results in 4.1 were extracted for Lisbon's TMA. As proof of concept, we ran the programs for Oporto. These results are in 4.2.

With the exception of 4.1.4, all the results were obtained using a 2 nautical miles buffer.

In Fig.9 is the colormap used to represent the percentage of adherence.

Figure 9: Colormap percentage scale.

4.1. Lisbon's TMA - LPPT

The set of results presented in this chapter attempts to portray all different scenarios. The aim is to be able to best compare and contrast all of them and conclude on the topic.

4.1.1 2D adherence, all data

The first test was the two dimensional adherence for all the data.

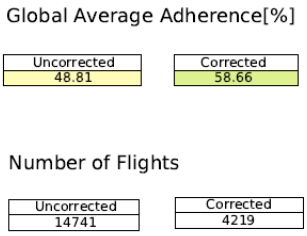

Figure 10: Global Average 2D Adherence for LPPT.

The uncorrected STAR's have an average global adherence of 49%. Assuming the corrections made reflect ATC's intervention, if the flight plan was updated during flight this adherence would increase to 59%. This is illustrated in Fig.10. In the 3 months analyzed, 18960 aircrafts flew into Lisbon's airport from which 4219 were corrected. In average, there were 206.1 flights per day.

From this point forward, unless mentioned, the results presented are for the corrected STARs.

4.1.2 2D vs 3D adherence

In this section a comparison is made between 2D and 3D adherences.

The global average adherences for 2D and 3D are presented in Fig.11.

(a) 2D (b) 3D

Figure 11: Global Average Adherence for 2D and 3D.

In Fig.12 come the tabulated adherences per STAR per segment, the 1st segment being the one closest to the runway.

The UNPOT3K STAR has 0.12% adherence in the first segment. This is explained by the very narrow corridor regulated for this STAR shown in Fig.13.

4.1.3 High vs low traffic scenario

A congested terminal area would suggest a higher percentage of adherence. During low traffic periods pilots have more freedom to fly directly without having to follow the specific path.

This study aimed to find the relation between airport's traffic and STAR's adherence. For this, taking the number of flights and the global average 3D adherence for each day, two graphs were produced. These can be seen on Fig.14: a) corresponds to the

	1	2	3	4	5	6	7	8	9	10	11	12
GAIOS3B	87.68	52.08	9.80	3.97	1.61	0.14	0.73	0.16	0.00	0.00	0.00	6.82
TROIA3B	91.49	71.31	30.40	4.24	0.80	2.18	2.70	8.71	5.15	3.08		
BUSEN3B	90.60	46.74	5.20	0.72	0.34	3.15	9.36	14.82	6.22	8.61		
NAKOS5A	86.16	73.97	37.88	5.24	12.13							
EXONA3B	89.69	63.18	12.70	6.28	14.82							
UNPOT3D	89.37	43.70	15.47	5.28	29.56	18.92	21.24					
NAKOS3B	90.95	61.30	9.34	3.47	1.97	1.43	11.02	56.38	23.73	15.24		
LIGRA3B	93.14	56.61	11.66	3.86	0.00	2.49	8.49	38.25	40.09	25.31		
GAIOS3D	91.43	50.93	6.95	2.54	49.86	26.17	20.92					
UNPOT5A	85.78	75.39	38.35	15.34								
LIGRA5A	90.51	91.55	21.95	21.86								
BUSEN3D	91.76	60.06	33.38	26.25	32.29	8.86	31.98					
UNPOT3B	95.41	60.98	13.07	5.19	3.94	4.65	16.32	25.20	37.84	61.05		
XAMAX6C	86.61	68.55	29.03	15.00	6.49	45.81	43.62					
XAMAX5D	92.46	68.65	41.77	23.20	36.35							
GAIOS5A	84.92	59.57	35.64	41.48	32.66							
XAMAX3B	91.79	83.43	50.97	20.08	27.70	42.87						
UNPOT3K	85.59	66.90	57.24	27.85								
TROIA3D	92.14	59.25	55.66	60.54	67.02	17.71	8.12					
BUSEN9P	86.44	63.15	33.09	41.94								
TROIA5A	86.37	54.04	45.37	37.83	8.21							
XAMAX5K	83.22	47.99	29.07	51.86	92.08	30.58	31.96					
EXONA5A	83.94	59.09	35.56	25.74	53.46							
IDBID5B	91.20	76.91	33.91	27.96	46.19	57.33						
XAMAX5A	89.85	88.42	59.24	47.56	69.26	87.73	92.23	31.97	30.96			
LIGRA3D	91.99	61.13	18.13	9.31	65.13	59.27	65.93					
INBOM3B	92.25	86.00	69.72	44.06	58.65	60.96						
NAKOS3D	92.18	64.11	51.63	29.05	74.15	64.59	78.50					
INBOM5A	84.93	60.15	21.49	13.85	26.01	62.26	91.62	86.00	67.43			
INBOM5K	84.06	53.98	37.24	58.27	92.66	85.74	78.58					

(a) 2D

	1	2	3	4	5	6	7	8	9	10	11	12
UNPOT3K	0.12	34.57	18.26	4.90								
GAIOS3B	86.28	35.46	9.80	3.97	1.61	0.14	0.42	0.00	0.00	0.00	0.00	6.58
BUSEN3B	89.16	36.97	5.20	0.72	0.28	1.50	3.00	3.40	6.09	8.14		
TROIA3B	90.75	63.41	30.34	2.60	0.48	1.48	0.06	5.11	5.10	2.96		
XAMAX5K	78.52	37.23	9.21	5.22	23.49	16.77	0.75					
NAKOS3B	90.14	52.35	9.34	2.72	0.80	1.07	3.12	28.12	23.27	14.93		
LIGRA3B	90.70	46.24	11.66	3.82	0.00	2.49	3.03	16.27	40.09	25.08		
NAKOS5A	86.10	68.04	35.70	5.07	11.97							
EXONA3B	89.43	58.22	12.70	5.49	14.45							
UNPOT3D	89.00	38.48	6.48	3.01	27.41	18.92	20.17					
INBOM5K	79.93	42.75	13.48	7.88	27.17	39.15	0.77					
GAIOS3D	91.44	40.71	0.00	2.31	44.98	26.17	20.92					
UNPOT5A	85.57	69.07	38.18	14.28								
UNPOT3B	91.38	57.11	13.07	4.07	1.89	1.86	4.13	13.75	35.66	57.22		
LIGRA5A	90.21	85.07	21.47	21.83								
BUSEN3D	91.44	55.93	15.97	19.15	30.02	8.86	29.97					
XAMAX6C	86.45	60.94	28.96	14.89	5.42	41.20	39.27					
TROIA3D	92.14	55.48	0.00	35.80	65.21	17.71	8.12					
XAMAX5D	92.22	65.92	30.38	19.54	34.66							
GAIOS5A	84.62	50.20	34.13	41.02	32.18							
XAMAX3B	91.77	80.99	50.91	19.85	27.53	41.25						
BUSEN9P	86.13	54.19	32.73	40.81								
TROIA5A	86.07	47.05	44.83	37.36	7.54							
XAMAX5A	89.68	81.52	59.24	47.02	68.39	87.20	90.74	28.47	12.73			
EXONA5A	83.75	51.82	34.46	25.60	51.19							
IDBID5B	91.01	74.01	33.90	27.30	42.33	40.99						
LIGRA3D	91.99	55.01	3.84	4.08	60.47	59.27	65.93					
INBOM5A	84.68	52.71	21.43	13.63	25.66	58.35	82.42	75.61	24.58			
NAKOS3D	90.77	55.14	20.00	19.89	65.66	60.02	76.32					
INBOM3B	92.08	83.38	69.72	42.98	57.92	56.38						

(b) 3D

Figure 12: Adherence per STAR per segment.

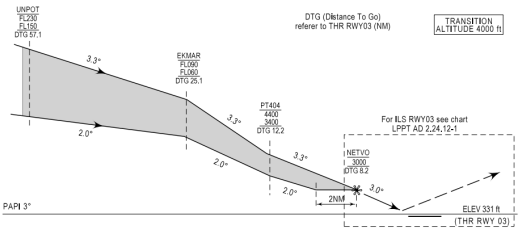

Figure 13: UNPOT3K altitude restrictions. [2]

global average adherence for the data without corrections and b) for the corrected data.

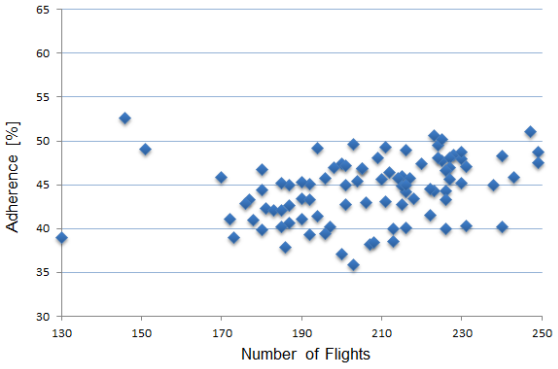

(a) Uncorrected

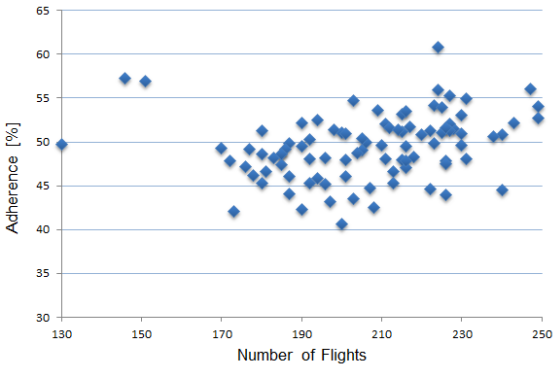

(b) Corrected

Figure 14: Number of flights per day vs adherence.

4.1.4 Buffer radius

Augmenting the buffer will evidentely increase STAR's adherence. The idea of this study was to find the best buffer, i.e. the buffer that produces better results without compromising accuracy.

We tested the adherence for the 3 months with the different buffer radius available: 1, 2, 3, 4 and 5nm. The results come in graph form presented in Fig.15. Each line corresponds to a different STAR and the graph confronts buffer radius with adherence.

The idea behind this graph was to visually calculate the area below each line and sequence the STARs by decreasing area. From top to bottom, on the figure, comes the sequence. Choosing the buffer would be a question of identifying which buffer produced the most similar sequence.

4.1.5 Average STARs

With the Average STARs test 3 different patterns were produced, one for each algorithm used. Fig.16 is an example of these patterns for the BUSEN3B

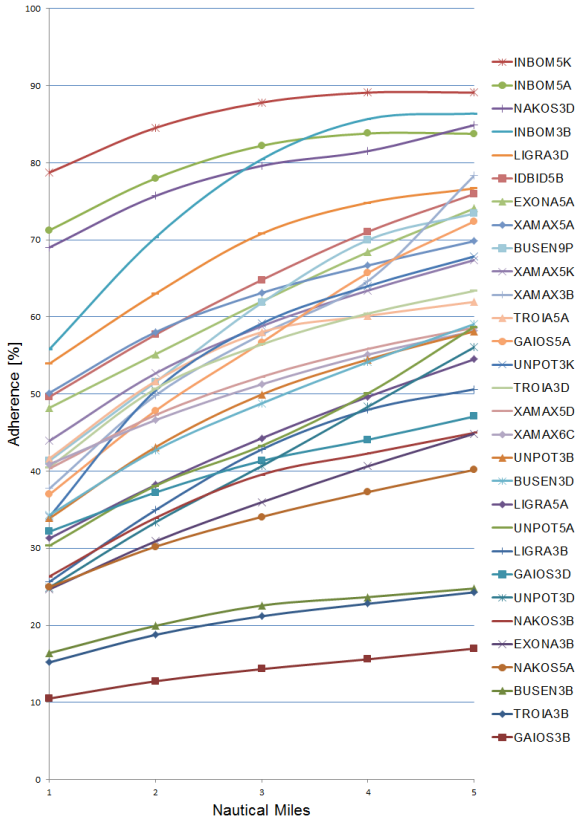

Figure 15: Buffer radius in nautical miles vs percentage of adherence.

STAR. The one in red is the Average, in green the Weighted Average and in dark yellow the Median. The blue one is the real STAR. Not all the tracks are presented in QGIS but all of them were used in the calculations. The tracks in grey are a sample of 50 of the tracks used in the calculations.

After obtaining these patterns, a comparison between each of the patterns and the real STAR was made, i.e. the adherence for each case. The results are presented in Fig.17.

The global results, accounting for all STARs come in Fig.18.

4.1.6 Point Direct

Studying the average STARs, scenarios like the one in Fig.19 were often found. In the image, the map on the left shows the real STAR and a sample of 50 tracks assigned to that STAR. On the right the 3 patterns obtained with the Average STARs test can be seen. For these STARs, the trajectory patterns are not best represented as lines. Here, the tracks come from a large cone shaped area of entrance and most often fly directly to a point along the STAR, closer to the runway.

Because of scenarios like these, a test was made to find how many of these tracks flew directly and

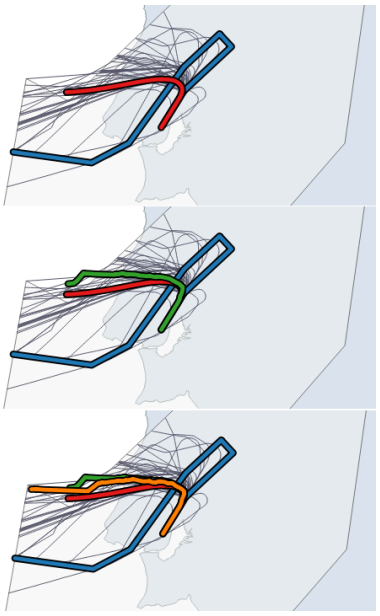

Figure 16: Average STARs for BUSEN3B.

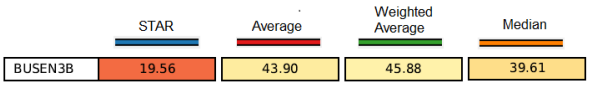

Figure 17: Adherence for each pattern route and STAR for BUSEN3B.

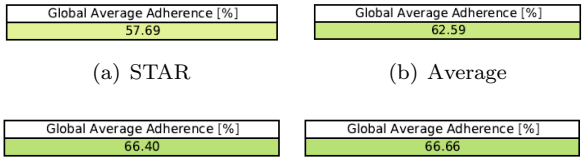

(a) STAR (b) Average

(c) Weighted Average (d) Median

Figure 18: Global Average Adherence for each pattern route.

Figure 19: Average STARs for NAKOS5A.

to what point of that STAR. The STAR in Fig.19 in particular had 771 non conformative flights, i.e. flights whose adherence was less than 70%. From these, 542 of them flew directly to NETVO, which corresponds to 70% of the flights. From the rest: 47 = 6% flew directly to PT404, 15 = 2% to PT406, and 18 = 2% to ADSAD. The name and location of

the STAR points can be consulted in Fig.20.

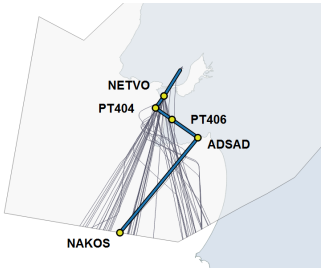

Figure 20: STAR points for NAKOS5A.

4.2. Oporto's TMA - LPPR

Adjusting the definition of the TMA sector, the STARs and the airport's elevation and altering the LPPT filtering point for LPPR, we were able to test the program's for Oporto's airport.

4.2.1 3D adherence, all Data

In the 3 months, there were 4962 flights landing in Oporto, which results in an average of 54 landings per day.

Firstly, the 3D adherence regarding all data was tested. The results are illustrated in Fig.21.

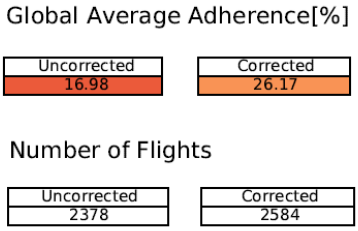

Figure 21: Global Average 3D Adherence for LPPR.

4.2.2 Distance Flown

As suggested by one member of the ATC at NAV, we wanted to make a test on mileage flown. For this we compared the length of the fixed paths with the length of the trajectories flown. The results come tabulated in Figs.22 and 23.

N° Flights	Distance Flown [nm]	STARs length [nm]	Mileage
4962	266879	300711	Savings of 11%

Figure 22: Total mileage savings.

The first shows the global results and the second discriminates between aircrafts that saved and aircrafts that spent more mileage. From the 4962

N° Flights	Distance Flown [nm]	STARs length [nm]	Mileage
4533 = 91%	238624	275355	Savings of 13%
429 = 9%	28255	25357	Spending of 11%

Figure 23: Discriminated mileage savings and spending.

flights, 91% saved mileage, i.e. if they had flown the STAR's fixed path as they were assigned to, they would have flown a bigger distance. In other words, it would have taken more time and more fuel would have been burnt.

5. Conclusions

There are multiple conclusions to be taken from this work:

- The adhesion of a flight to its flight plan STAR is, in average, 49%. Had this information been updated during flight, the adherence would increase 10% for 29% of the flights. Regarding the segmented STAR, the increase in adherence with distance to the runway is clear. The adhesion to the first segment is, in average, 87% and the last 25%. For the corrected test these numbers increase to 89% and 34% respectively. The QGIS platform is a big advantage on this study. It gives a visual perception of the width of the buffer and where the tracks fail to adhere the most.
- The 3D adherence results are an average of 9% lower than the 2D. The tables in Fig.12 show no clear relation between the segment order and the difference between 2D and 3D. Neither is there a relation between the STAR overall adherence and its difference in adherence between 2D and 3D. However, the geographical visualization of the 3D results show that this difference is notorious in the last segment: an average of 8%. Frequently the aircrafts enter the TMA at a higher altitude than the one regulated but quickly descend and return to path. On the other hand, the difference in adherences for the first segment is in average less than 1% (excluding the special case of UNPOT3K). At this stage the aircrafts are on the ILS path and don't deviate from it.
- The high vs low traffic scenario graphs show that there is no relation between the number of flights per day and the adherence to the STARs. Either with corrected or uncorrected data, no linear pattern could be extracted from the graphs.
- The buffer radius test led to the conclusion that a 2nm buffer was the best choice.

- The Weighted Average and the Median provide very similar values of adherence, 66% and 67% respectively. The Average provides 62.59% of adherence, a lower value, as expected. All of them allow for an increase in adherence, in comparison to the 58% adherence to the real STAR.
  Fig.16 shows that the pattern trajectories are generally simpler and more direct shortcut versions of the real STAR. Also, the Weighted Average and the Median produce very similar lines and therefore have similar results in adherence.

- Analyzing the direct-to flights for the STAR in Fig.19 concluded that 80% of the non conformative flights flew directly to a STAR point. The points with the biggest percentage of directs are the ones closest to the runway, i.e. the first point in line with the final approach ILS. However, this test does not apply for all the STARs. Some STARs, although having several non conformative flights, these do not fly directly to any particular point. For instance the XAMAX6C has 1380 flights, from which only 12% are directs. Besides being a small percentage it also is mainly for the two last STAR points, which makes this study not relevant for this case.

- The study for the TMA sector of Oporto shows that the corrections translate in an increase in adherence of 11%, similar to Lisbon. However, in this airport the average adherence in 3D was only of 26%, about 20% less than in Lisbon.

- Regarding distances, by not adhering to the STARs, there is an average savings of 11% of mileage flown per flight. The discriminated values show that only 9% of the flights are flying a bigger distance than they would if they were following the STAR. Considering constant speed, the relative error in time would equal the one in distance. Then, the ETA calculated by AMAN would have, in average, an error of 11% just for the TMA sector.

5.1. Achievements

Three main methodologies were developed to evaluate arrival procedures. The first one tests flight's adherence to a route. The second method traces trajectory based patterns from surveillance data. And the third one finds the incidence of direct flights and also extracts patterns from these incidences.

A set of programs to perform these methods was developed. Regarding adherence, two programs were created to test adherence to the STARs, one for 2D and one for 3D. A different program takes radar data and traces common trajectories forming alternative routes. Three alternative routes are obtained for each STAR, each following a different algorithm. Taking the 2D adherence test, a third adherence program was created with the distinctive option of choosing the route we are testing adherence on. This was built in order to evaluate and compare the alternative routes obtained earlier. Another program provides, for each STAR, the percentage of direct flights to each of its STAR points. All the tests have external programs solely for creating visual results. This includes the creation of PDF and QGIS files. Furthermore, an additional feature of correcting STARs was installed.

We quantified 2D and 3D adherence and, by comparison, were able to find where the 3D was lacking. A relation between amount of traffic and adherence was sought. The best buffer radius to use in the different tests was found. The alternative routes were extracted for every STAR and their adherences were compared among them and with the raw STAR. Direct flight's incidence for each STAR and each STAR point was found. The programs were tested for two different airports as proof of generality. The 3D adherence was tested for the second airport and compared between the two. Lastly, a test was made on distance flown, spendings and savings.

This work has already triggered some discussion among workers at NAV Portugal. Members of the ATC team showed great appreciation for it. Techniques such as vectoring, change in STARs and granting direct flights are daily practices. Still, the way this information is now available is a valuable asset on traffic flow's analysis. Moreover it is a refreshing view on these practices. Meetings have started to take place and are to be continued. This work is assisting and expediting the proccess of designing the optimal solution for the TMA sector in Lisbon.

5.2. Recommendations

For AMAN to be ready to be fully integrated into the system, the latter needs some improvements. A personal suggestion would be to undertake Point Merge and reduce the number of merging points to a minimum.

A final test was conducted for Lisbon's TMA to support the Point Merge undertake. The STARs were divided in 4 groups according to their assigned runway (RWY) and origin: North or South of the TMA. All the Median routes obtained with the Average STARs program were gathered and divided into the same groups.

The STARs and respective Median routes from

these 4 groups are shown on Figures 24, 25 and 26. On the left are the STARs, in blue, and on the right the Median routes in green.
Fig.24 shows that the way these STARs are structured already indicates two stand out merging points: PT414 and ADSAD. The Median routes, traced from real trajectories, confirm that there is already a tendency to merge the flights. Not only that, but also there is a tendency to further direct the flight into just one merging point: NETVO.

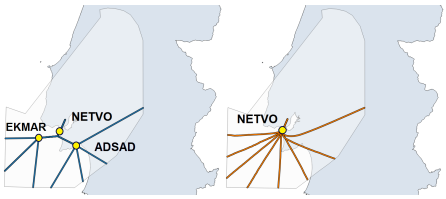

Figure 24: STARs and respective Median routes for RWYs 3/35, from the South.

Similarly to 24, Figures 25 and 26 also show promising merging points in the STAR structure on the left but one clear stand out effective point on the right.

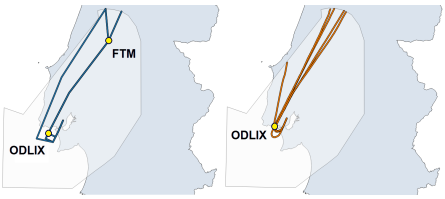

Figure 25: STARs and respective Median routes for RWYs 3/35, from the North.

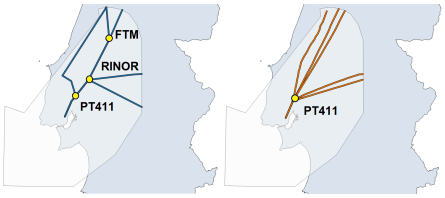

Figure 26: STARs and respective Median routes for RWY 21, from the North.

Lisbon's TMA has every visible condition to proceed with Point Merge. Not only do STAR's paths already indicate merging points but also the median proves that aircrafts do in fact merge into points. Figures show that merging points can be reduced and paths can be simplified.

5.3. Future Work
A proposal for future work would be to downsize the minimum scale of results, i.e. instead of the minimum being one day, make it hours or smaller time periods like morning, afternoon and evening. That would give us an idea of how the slots are distributed throughout the day and a relation between number of flights and adherence could then be extracted.

A second proposal would be the development of methods and algorithms capable of infering alternative STARs through 3D surveillance data.

Presenting results for every airport in Portugal would possibly initiate the idea of a TMA restructuring nation wise.

Lastly, and for the reasons presented in 5.2, a future development on the Point Merge study is suggested.

Acknowledgements
This thesis was developed under a protocol established between NAV Portugal and Instituto Superior Técnico. The author would like to thank the staff at the DEP/ATM department at NAV. Particularly José Vermelhudo for sheltering the work and Paulo Monteiro for his guidance. Ph.D. Prof. Rodrigo Ventura at IST for making the internship possible and choosing the author as the intern.

References
[1] Lisbon's FIR Traffic Evolution in June 2015.

[2] eAIP Portugal. Technical report, NAV Portugal, 2015.

[3] EUROCONTROL Agency. *Local Single Sky Implementation (LSSIP) Portugal, Year 2014 - Level 1.*

[4] S. Gillies. *The Shapely User Manual*, 1.2 and 1.3 edition, December 2013.

[5] N. Hasevoets and P. Conroy. *AMAN Implementation GUIDELINES.* EUROCONTROL Agency, 0.1 edition, December 2010.

[6] S. J. Zelinski and J. Jung. Arrival scheduling with shortcut path options and mixed aircraft performance. Presented at the Tenth USA/Europe ATM Research and Development Seminar (ATM 2015), June 2015.